Supplementary Information

Supplementary Materials and Methods

Mouse strains

The *Prox1*$^{fl/fl}$ and *Nkx2.5*$^{Cre/+}$ mouse strains used have been described previously (1, 2). The *Myf5*$^{Cre/+}$ (B6.129S4-*Myf5*$^{tm3(cre)Sor}$/J) was obtained from The Jackson Laboratory. *Prox1*$^{fl/fl}$ mice were crossed with Cre lines to generate *Prox1*$^{fl/fl}$ (control), Cre;*Prox1*$^{+/+}$ (cre), Cre;*Prox1*$^{fl/+}$ (het), and Cre;*Prox1*$^{fl/fl}$ (mutant) embryonic and adult mice. All animal experiments were carried out according to UK Home Office project licences compliant with the UK Animals (Scientific Procedures) Act 1986 and approved by the University College London Biological Services Ethical Review Process. Animal husbandry at UCL Biological Services was in accordance with UK Home Office Certificate of Designation.

Histology and immunofluorescent staining

Heart samples were fixed in 4% formaldehyde and embedded in either paraffin wax or OPT (both Raymond Lamb), and sectioned at 15 or 10 µm intervals, respectively. Sections were stained with haematoxylin (Sigma) and eosin (Raymond Lamb). Immunofluorescence staining was carried out on Triton-X (Sigma) permeabilised cryosections blocked with 0.1% BSA (Sigma) and 1% goat serum (Sigma). Prox1 (goat anti-rabbit, 1 in 200 dilution, AngioBio and rabbit anti-human, 1 in 200 dilution, ReliaTech), α-actinin: (goat anti-mouse, 1 in 200 dilution, Sigma), secondary antibodies: AlexaFluor 488/594 (1 in 200 dilution, Invitrogen). Skeletal muscles were removed and snap-frozen in OCT in isopentane cooled in liquid nitrogen. Serial cross sections of muscle were cut at 10 µm intervals. Fiber-type staining was carried out on unfixed tissue using antibodies from the Developmental Studies Hybridoma Bank. Prox1 immunofluorescence with fiber type counterstaining and wheat-germ agglutinin conjugated

to alexafluor 594 (Invitrogen) staining were performed on fixed tissue. Sample analysis was carried out using a Zeiss Imager Z1 microscope with an AxioCam MRm camera attachment running AxioVision software release 4.8 (all Carl Zeiss). Prox1 and α-actinin staining on heart sections (Fig. S1) and skeletal muscle sections (Fig. 4A and Fig. S7) were imaged using a Zeiss LSM 710 confocal microscope. Image processing and quantification analyses were performed using ImageJ.

Quantitative real-time (qRT) PCR analysis

Total RNA was extracted from frozen tissue samples using TRIzol reagent (Invitrogen), with DNA contaminants removed using the RQ1 RNase-Free DNase kit (Promega). Alternatively, where tissue sample size was limiting, total RNA extraction and DNAse treatment was carried out using the RNeasy Mini Kit (Qiagen). Reverse transcription was performed using SuperScript III Reverse Transcriptase (Invitrogen). qPCR analysis was performed on an ABI 7000 Sequence detector (Applied Biosystems) using SYBR Green (Applied Biosystems). Data was analysed in Excel where gene expression was normalised to *Hprt1* expression and presented as fold change.

Primer sequences are as follows:

qRT-PCR primers used with SYBR® Green reagents		
Gene (Mouse)	**Forward**	**Reverse**
ANF	GCTTCCAGGCCATATTGGAG	GGGGGCATGACCTCATCTT
BNP	GAGGTCACTCCTATCCTCTGG	GCCATTTCCTCCGACTTTTCTC
Hprt1	TCAGTCAACGGGGGACATAAA	GGGGCTGTACTGCTTAACCAG
Myh1	CTCTTCCCGCTTTGGTAAGTT	CAGGAGCATTTCGATTAGATCCG
Myh2	ACTTTGGCACTACGGGGAAAC	CAGCAGCATTTCGATCAGCTC
Myh4	CTTTGCTTACGTCAGTCAAGGT	AGCGCCTGTGAGCTTGTAAA
Myh6 (α)	GCCCAGTACCTCCGAAAGTC	GCCCTTAACATACTCCTCCTTGTC
Myh7 (β)	ACTGTCAACACTAAGAGGGTCA	TTGGATGATTTGATCTTCCAGGG
Myl1	AAGATCGAGTTCTCTAAGGAGCA	TCATGGGCAGAAACTGTTCAAA
Prox1	GAAGGGCTATCACCCAATCA	TGAACCACTTGATGAGCTGC
Sox6	ACGTCTACCTCACCACATAAGC	CGGGGTTCCAAAAGTAACACT
Thrap1	CGACTTGACAGGAATTAAGTGGA	GGAAACAGAATAGGGGCGGAA
Tnni2	AGAGTGTGATGCTCCAGATAGC	AGCAACGTCGATCTTCGCA
Tnnt3	GGAACGCCAGAACAGATTGG	TGGAGGACAGAGCCTTTTTCTT

Chromatin immunoprecipitation (ChIP)

Chromatin was prepared from age- and sex-matched hearts from 8-12 weeks old control (Co, *Prox1*$^{fl/fl}$; N>4) and mutant (Mut, *Nkx2.5*$^{Cre/+}$; *Prox1*$^{fl/fl}$; N=3) mice. Hearts were dissected in chilled PBS; minced and fixed with 1% formaldehyde solution at room temperature, and quenched with 0.125 M glycine before washing twice with PBS supplemented with protease inhibitors (Protease Inhibitor Cocktail Tablet (Roche), 1 mM PMSF (Sigma) and 1 µg/mL aprotinin (Sigma)). Cells were then lysed (10 mM EDTA, 50 mM Tris-HCl (pH 8.0), 1% SDS, protease inhibitors). Chromatin was sonicated to generate fragment sizes of 500-1000bp, and immunoprecipitated using antibodies for Prox1 (ReliaTech, 102-PA32; AngioBio, 11-002), HDAC1 (Abcam, ab7028), HDAC2 (Abcam, ab7029), HDAC3 (Abcam, ab7030), or control IgG (Abcam, ab46540). Isolation of immunoprecipitated chromatin was done according to manufacturer's protocol (Millipore). The amount of specific immunoprecipitated DNA was then quantified by qRT-PCR, with each reaction performed in triplicate. Signals from individual

ChIP reactions were used to calculate the % recovery of a given DNA segment relative to the total input signal. These values were then normalized to IgG ChIP signals to determine relative enrichment in Prox1, HDAC1, HDAC2 or HDAC3 antibody immunoprecipitated DNA over IgG. PCR primers used to detect the ChIP regions within *Tnnt3* are in Fig. S3. Those for *Tnni2* and *Myl1* have been previously published (3, 4) .

Statistical methods

Values are presented as +/- SEM. Gene expression determined by qRT-PCR was normalised to *Hprt* levels and represented as relative change. Statistics were calculated in Excel using Student's t-test unless otherwise stated. *P*-values <0.05 were considered statistically significant (* = $P<0.05$, **= $P<0.01$, ***= $P<0.001$, ****= $P<0.0001$). Quantification of western blots carried out using ImageJ and normalised to GAPDH levels. Significant deviation from expected Mendelian ratios was calculated in Excel using Chi-Squared tests.

Affymetrix Microarray

Microarray analysis was carried out as previously described (5). Briefly, E12.5 hearts from cardiac-specific *Prox1* knockouts were compared to stage-matched controls using Affymetrix Mouse Exon 1.0ST arrays. Data was processed using Affymetrix expression console software and analysed in Partek.

Magnetic Resonance Imaging (MRI)

Mice were anaesthetised and placed onto an animal cradle. Oxygen and isoflurane (1-2%) were provided via nose cone. A water-heating system and heated air blower were used to

maintain body temperature. A neonatal apnoea pad was used for respiration gating and subcutaneous electrodes were used for electrocardiogram (ECG) gating.

Imaging was performed using a 9.4T Agilent (Santa Clara, US) scanner with a 39mm volume coil (Rapid MR International, Rimpar, Germany). A double-gated spoiled gradient echo sequence was used to acquire cine cardiac images which were used to calculate ejection fraction (EF) and normalised left ventricular mass (nLVM). Imaging parameters were TR = 5ms, TE = 1.1ms, flip angle = 15°, slice thickness = 1mm, matrix size = 128 x 128, FOV = 25.6 x 25.6 mm. 8-12 slices were acquired from apex to base of the heart. To visualise thrombi, late gadolinium contrast agent enhanced MRI was performed as described elsewhere (Price et al., 2011). In brief, 0.6 mmol/kg Gd-DTPA (Magnavist, Schering AG, Germany) was injected through an intra-peritoneal infusion line. After an 8 minute delay to allow contrast agent to circulate, an inversion recovery gradient echo sequence was used for high SNR between the blood pool and thrombi. Imaging parameters were as above except for: TR = 3.1ms, flip angle = 90°, TI = ~4 x RR-interval. Aorta diameter was measured at 5 points in a 4 chamber, long axis CINE image.

Western blotting

Heart and skeletal muscle samples were lysed in RIPA buffer (50 mM Tris-HCl at pH7.6, 150 mM NaCl, 1% NP-40, 0.5% DOC, 0.1% SDS) supplemented with protease inhibitors (Protease Inhibitor Cocktail Tablet (Roche), 1 mM PMSF (Sigma) and 1 µg/mL aprotinin (Sigma)). The lysate was centrifuged at 13,000xg for 15 min at 4°C and the supernatant recovered. For SDS-PAGE, samples were incubated with an equal volume of 2 x Laemmli Buffer/5% β-ME at 95°C for 5 min, before being resolved on a 10/15% acrylamide gel (Sigma) and analysed by Western blot using a primary antibody for Prox1 (rabbit anti-human, 1 in 1000 dilution, ReliaTech), β-

MHC (goat anti-mouse, 1 in 2000 dilution, Sigma), Type I (BA-D5-s), Type IIa (SC-71-s), Type IIb (BF-F3-s), Type I, IIa and IIb (BF-35-s; all Developmental Studies Hybridoma Bank) or GAPDH (goat anti-mouse, 1 in 1000 dilution, Millipore). All secondary antibodies conjugated to HRP and imaged using enhanced chemiluminescence (all GE Healthcare).

Silver staining of high resolution polyacrylamide gels

Protein extraction and silver staining of gels was carried out as described (6) Briefly, protein was extracted from freshly frozen muscle tissue in extraction buffer (0.3 M KCl, 0.1 M KH_2PO_4, 50 mM K_2HPO_4, 10 mM EDTA, pH 6.5) with Complete protease inhibitor cocktail (Roche). Protein extracts were diluted 1:1 (vol/vol) with 60% glycerol. 0.1 μg of protein was separated on an 8% polyacrylamide gel with a 4% stacking gel, each containing 30% glycerol. The gels were run at 4°C for 48 h at 70 V. Following electrophoresis, the gels were silver stained with SilverQuest^{TM} staining kit (Invitrogen).

Succinate dehydrogenase staining

Frozen sections of skeletal muscles (10 μm) were stained for succinate dehydrogenase (SDH) activity to determine the oxidative capacity of the muscle fibers, as described previously(7).

Muscle tension experiments

Isometric muscle tension physiology was performed on male control (*Prox1*$^{fl/fl}$), cre (*Myf5*$^{Cre/+}$), het (*Myf5*$^{Cre/+}$; *Prox1*$^{fl/+}$) and test mutant (*Myf5*$^{Cre/+}$; *Prox1*$^{fl/fl}$) mice aged 10 weeks. Briefly, under deep anaesthesia (4.5% chloral hydrate (Sigma), by IP injection), hind limbs were immobilized and the distal tendons of the soleus and EDL muscles of both hind limbs exposed and attached to force transducers. Sciatic nerves were then exposed and severed at

mid-thigh level with the distal stumps placed in contact with stimulating electrodes. Time-to-peak and half-relaxation times were recorded following square wave stimuli of 0.02ms duration. Values were determined for individual muscles using a Picoscope^{TM} oscilloscope and software and averaged for each genotype. Tetanic contraction was induced by delivering trains of stimuli at 40, 80 and 100Hz for 2.5s duration, to induce the maximal contractile force, with values determined as previously. Fatigue traces for soleus muscles were obtained by stimulating muscles repeatedly over a 3 minute period with the resultant decrease in contraction amplitude recorded over time using a pen recorder.

Supplementary References

1. Harvey NL*, et al.* (2005) Lymphatic vascular defects promoted by Prox1 haploinsufficiency cause adult-onset obesity. *Nat.Genet.* 37(10):1072-1081.
2. Moses KA, DeMayo F, Braun RM, Reecy JL, & Schwartz RJ (2001) Embryonic expression of an Nkx2-5/Cre gene using ROSA26 reporter mice. *Genesis.* 31(4):176-180.
3. Montgomery RL*, et al.* (2007) Histone deacetylases 1 and 2 redundantly regulate cardiac morphogenesis, growth, and contractility. *Genes Dev.* 21(14):1790-1802.
4. Niro C*, et al.* (2010) Six1 and Six4 gene expression is necessary to activate the fast-type muscle gene program in the mouse primary myotome. *Dev.Biol.* 338(2):168-182.
5. Rossdeutsch A, Smart N, Dube KN, Turner M, & Riley PR (2012) Essential role for thymosin beta4 in regulating vascular smooth muscle cell development and vessel wall stability. *Circ Res* 111(4):e89-102.
6. Oh M*, et al.* (2005) Calcineurin is necessary for the maintenance but not embryonic development of slow muscle fibers. *Molecular and cellular biology* 25(15):6629-6638.
7. Kieran D & Greensmith L (2004) Inhibition of calpains, by treatment with leupeptin, improves motoneuron survival and muscle function in models of motoneuron degeneration. *Neuroscience* 125(2):427-439.

Table S1: Top ten hits from microarray comparing gene expression in cardiac-specific *Prox1* knockout and control hearts at E12.5

	P-value	Symbol	Gene Name	Function
1	1.04E-08	***Tnnt3***	*Troponin T3, skeletal, fast*	fast-twitch skeletal muscle isoform component of the troponin complex, regulates striated muscle contraction
2	5.75E-08	***Tnni2***	*Troponin I, skeletal, fast*	fast-twitch skeletal muscle isoform component of troponin complex, regulates striated muscle contraction
3	1.33E-06	***Myl1***	*Myosin, light polypeptide 1*	fast-twitch skeletal muscle isoform, regulates striated muscle contraction
4	1.14E-05	***Tm6sf***	*Transmembrane 6 superfamily*	integral to membrane
4	1.14E-05	***Hdgfrp3***	*Hepatoma-derived growth factor, related protein 3*	chromatin binding, growth factor activity, cell proliferation
5	2.11E-05	***Casq1***	*Calsequestrin 1*	calcium binding, regulation of muscle contraction
6	4.40E-05	***Cck***	*Cholecystokinin*	DNA binding, protein binding, neuropetide hormone activity
7	5.25E-05	***Adamdec1***	*ADAM-like, decysin 1*	hydrolase activity, metallopeptidase
8	7.00E-05	***Nmb***	*Neuromedin B*	neuromedin B receptor binding, glucose homeostasis, neuropeptide signalling pathways, cell proliferation
9	7.80E-05	***Unc119***	*Unc-119 homolog (C. elegans)*	lipoprotein transport, myofibroblast differentiation
10	8.77E-05	***Abra***	*Actin-binding Rho activating protein*	actin binding, transcription coactivator activity, positive regulation of Rho signal transduction, actin cytoskeleton, myofibril, sarcomere

Supplementary Figures

Fig. S1. Myofibril disarray in adult *Prox1* mutant hearts. Immunostaining for α-actinin and Prox1 on sections through control (Co) and mutant (Mut) adult hearts. Nuclear Prox1 expression is lost in mutant hearts and is associated with myofibril disarray, revealed by aberrant α-actinin localisation and loss of striation. Scale bar 50 μm (left), 10 μm (right).

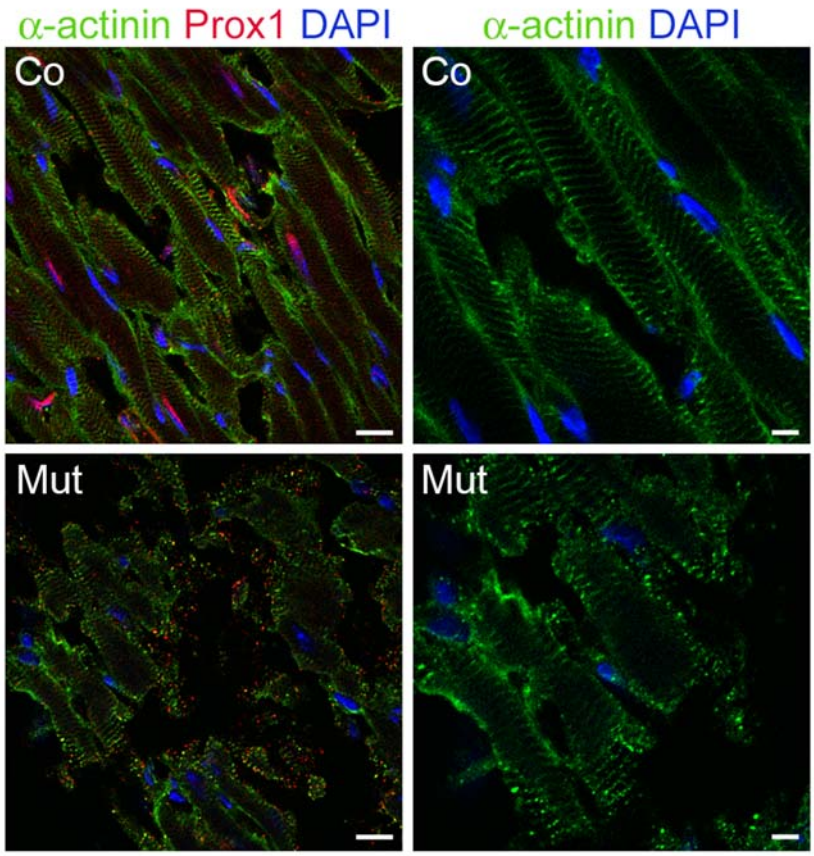
α-actinin Prox1 DAPI
α-actinin DAPI
Co
Co
Mut
Mut

Fig. S2. Mild ventricular septal and tricuspid valve defects in *Prox1* mutant adult hearts. Hematoxylin and eosin stained frontal sections through control (Co; A and B) and mutant (Mut; C, D and E) adult hearts. The membranous portion of the ventricular septum was aneurysmal (black asterisks; compare B with C and D) and there was thickening of the tricuspid valve leaflets in all mutant hearts examined (black arrows; compare A with C). In 20% of mutant hearts there were imperfections in the muscular ventricular septum (E). These defects are consistent with those observed during embryogenesis but are less severe and, therefore, compatible with survival beyond birth. Scale bar 500 μm and 50 μm.

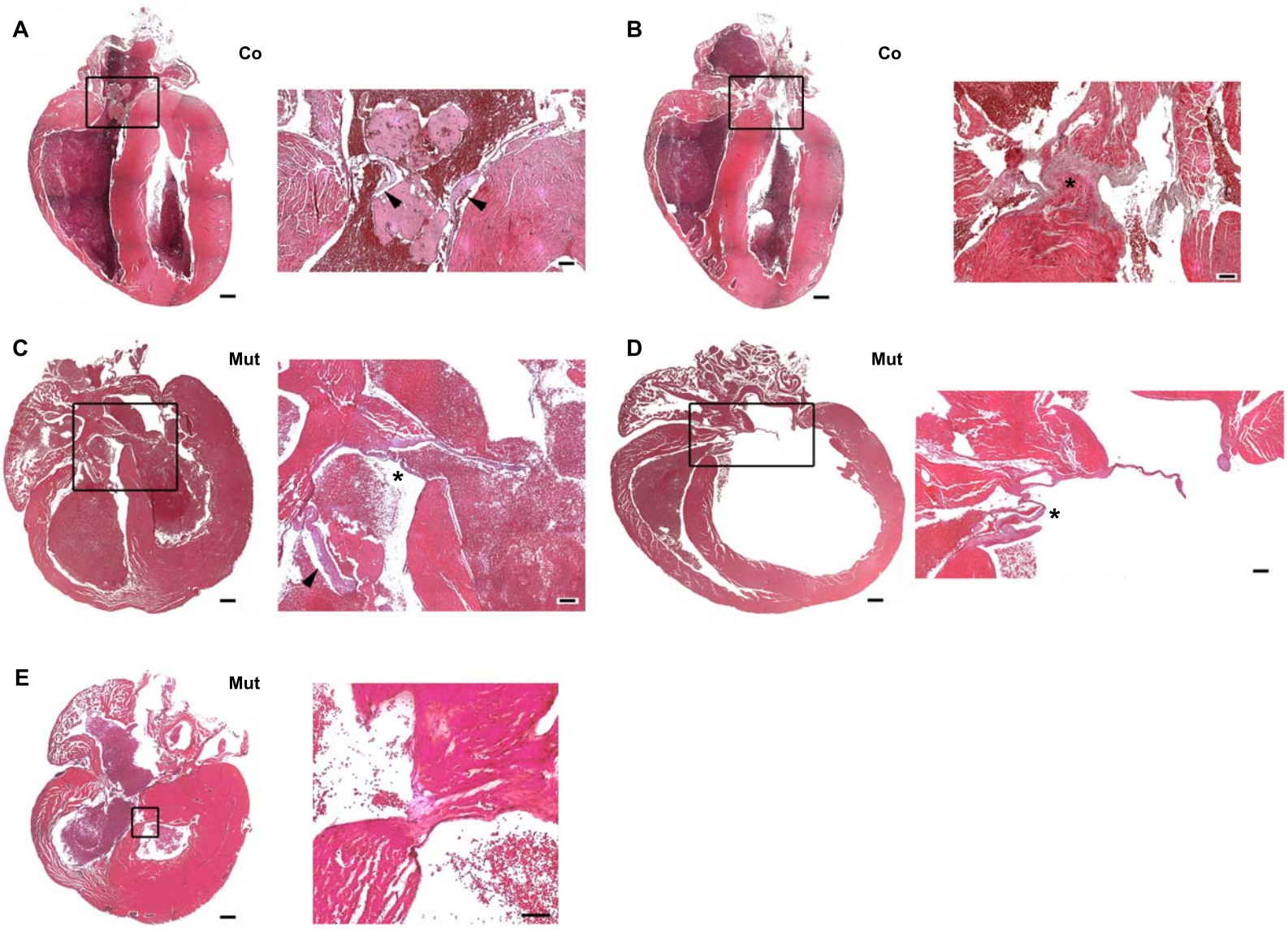
A
Co
B
Co
C
Mut
D
Mut
E
Mut

Fig. S3. Determination of conserved regions for *Tnnt3* ChIP. (**A**) Location of evolutionarily conserved regions within *Tnnt3* genome (www.mulan.dcode.org), with areas of interest marked with an arrow. (**B**) Section of *Tnnt3* genomic sequence (NCBI) beginning with Exon 1 (bold) labelled with region used on original ChIP-on-chip (yellow), first evolutionarily conserved regions from (**A**) (red underline) and location of primers used for ChIP which share the middle primer sequence (green).

A

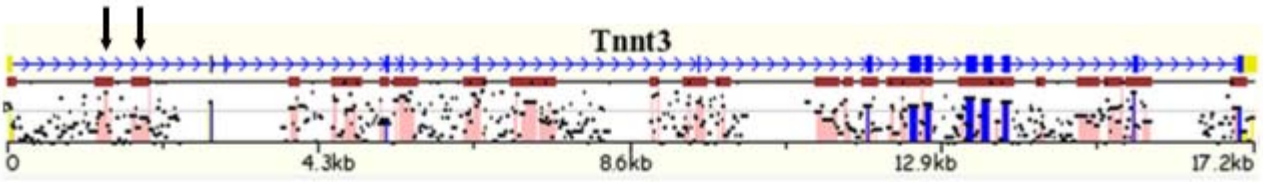

B

GGACAGTGCCTGCTGCTGGTCCTGTCCACAAGGAGCCCCCAGCCTTTCTCAGACTCAACT
ACAGGTGTGTATGGATGTGAACAGCCCGCGTAGGAGTGGGCAACTGTGTCTGGGCTTGGC
TGCCTAGCATCTAAGGGGAGTTCAATGGGTCCTGTGCCTCTTGCTGTGTTGTATTTTGGTAA
CTAGAAGCATGGTGCTTGAACCTTGGGATGACATAAAAGATCTGGTTCTAAACCAGAATAG
AAAAGCACAGGAAGTGAGAAGGAGTGGGGCTCCTGTGTGACTCAGGACAAAGGAGACC
TCCTAAGGTAGGATCTAGGAAGAAGGGCAGAGGGTGAGATAAGGATCGAGTGAGTCAGA
GGACATCATTCAGAGCTCTAAGGGCGCCTGCAGCTGCCTGCCTGGCAGCTGGCTGGAGCC
CCTCTGAGACTCTGAAAGAATGACCTTAGAGAAAGAATGTGATTTCAACTCATCCTTGGAG
CCCATGGGTCTGCCCTTTTGCAGATCTGGGCTTATCTCAGATCACCCTGGGAAGAAGCTCA
GGGGAGAGATATCTGTGAACCCCTGGGGCAGATTCCTAAGGTTCAGGTGAAGACAAACA
GGAGCCAAGCTGAACCAGGACAGAGGGAATGAAAGGAGCCTGGGCCTGAGCAGGAAG
CTCATATCTGATCTTGTGGCTGGGAGACCAGGTGGCCCCTAGCCCTCCAGGCTCCCGCCTT
TGTTAAGTTGCCGGGCTGGGATTCCTAACTTCCTGAGTTGAACTTTCTAGATGTCCTTGGG
AATCCTTGGAGGAAACCGGACCTAGCAAGGTTGTTCAGAGCAGACTAGGCCCAAAGCAG
GAAGTGATAAGGGACCCATAGCAAGTGAGTGGCAGGGCCCCCTGCCCCTTTTTGGCCTTT
GTCACCTTTGAAGGAAAGGAGTTTGGCATGGATCCCCAAGGAAACTGACCTCACAGGCTA
TTTTTGTGAACCTTCTTCTAAGCCCAGAACCCTCTACAGAACAACTGTTTTCACTCTCTGTT
GTTTATTGGTCATCTCTGTCCCATCCCTGACACCCCACCTCTGCCTCTCCCCAATTTATAGAA
ATGTTGAAATGGGGGTGGAGATGCACAGATATGCTCAAGTGGGCCTTCTGGACCTCTTTAG
AAGACCAGGAACCTCAGTTTCTCAACCTCAAACAAGGGCATTGCTACCTCACTTTGGAAG
GGTACAAGGCTGCCCTTGCTGGATGGATGCCTTTAGGAGCCAGGAGGGGAGCCAAGATG
GCTAGGTTGTTCTCAGTACCCTGCCCCCCTGCCATCTTGGGTTTCAGGGCAGAGGAGTCTT
GCTAATTTTGATGCCTATTTTTGGACACTTCAGCTGCCACTGGCTCCTTATAAACGCATGAC
ACCCCATGCAAACACACTACCCCTCCCTCCACTGCTGACAGGTGTGTGGGTCCAGTAGAAA

Fig. S4. HDAC binding to putative regulatory regions within *Tnnt3* and *Myl1* are altered in *Prox1* deficient hearts. ChIP-qPCR quantification of HDAC1 (**A**, **D**), HDAC2 (**B**, **E**) and HDAC3 (**C**, **F**) antibody-immunoprecipitated chromatin from adult hearts of control (*Prox1*$^{fl/fl}$; N=6; white bars) and mutant (*Nkx2.5*$^{Cre/+}$;*Prox1*$^{fl/fl}$; N=3; black bars) hearts using primers targeting responsive elements within Tnnt3 (**A**-**C**) and Myl1 (**D**-**F**) genomic loci. ChIP-qPCR signals were standardized to the % of input DNA and normalized to IgG ChIP signals to determine the relative enrichment of anti-HDAC1, HDAC2, or HDAC3 antibody over IgG immunoprecipitated chromatin. Each ChIP-qPCR reaction was performed in triplicate. Loss of binding in mutant hearts determined by Student's t-test comparison to control heart chromatin; ns, not significant; *p≤0.05 and **p≤0.01.

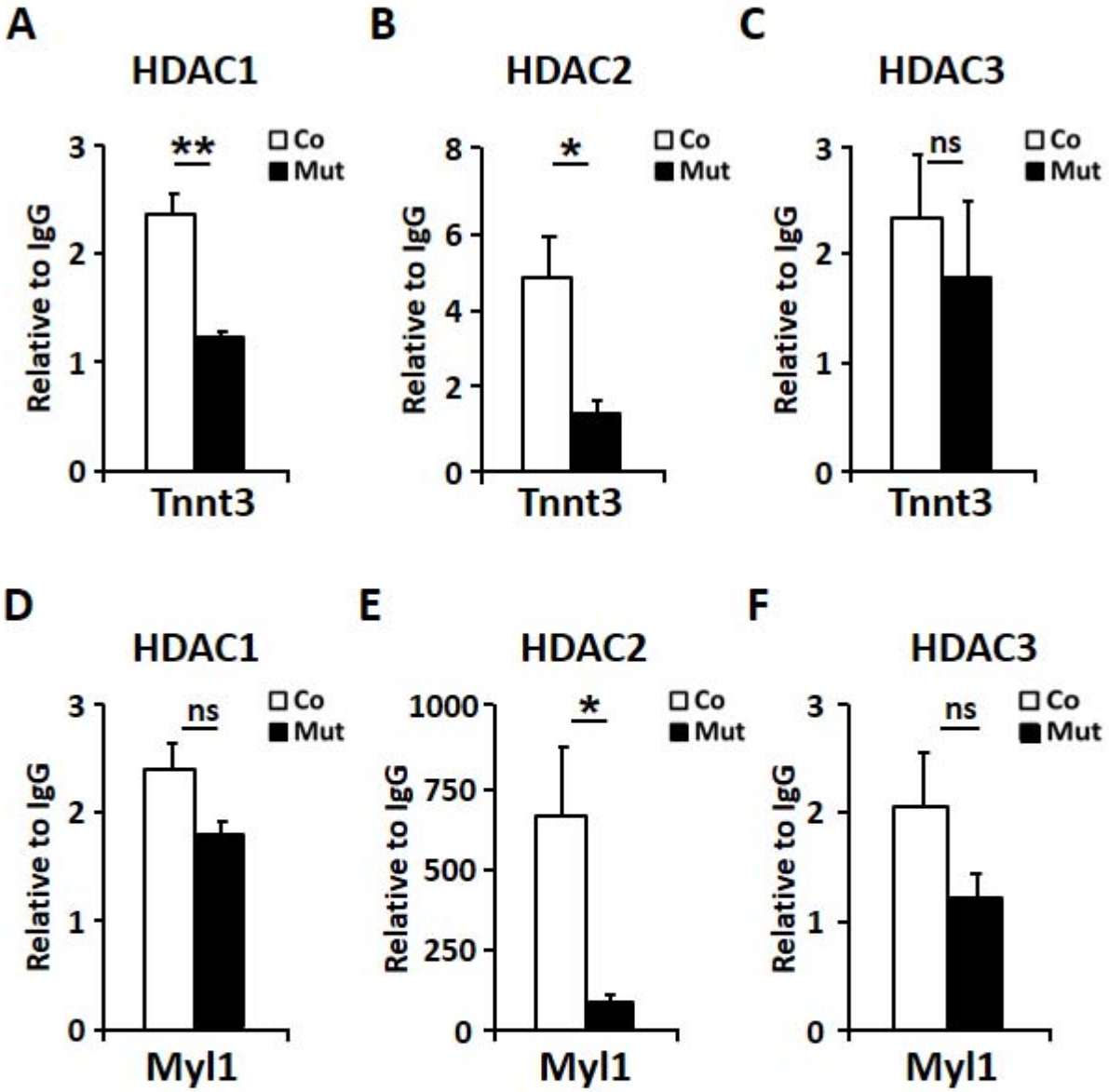
A
HDAC1
**
Co
Mut
Relative to IgG
3
2
1
0
Tnnt3
B
HDAC2
*
Co
Mut
Relative to IgG
8
6
4
2
0
Tnnt3
C
HDAC3
ns
Co
Mut
Relative to IgG
3
2
1
0
Tnnt3
D
HDAC1
ns
Co
Mut
Relative to IgG
3
2
1
0
Myl1
E
HDAC2
*
Co
Mut
Relative to IgG
1000
750
500
250
0
Myl1
F
HDAC3
ns
Co
Mut
Relative to IgG
3
2
1
0
Myl1

Fig. S5. No aortic stenosis in Prox1 mutant hearts. (**A**) The diameter of the aorta was measured at five points (a-e) in a four chamber, long axis CINE image. (**B**) There were no significant differences in aortic diameter between control (N=6) and mutant (N=4).

A

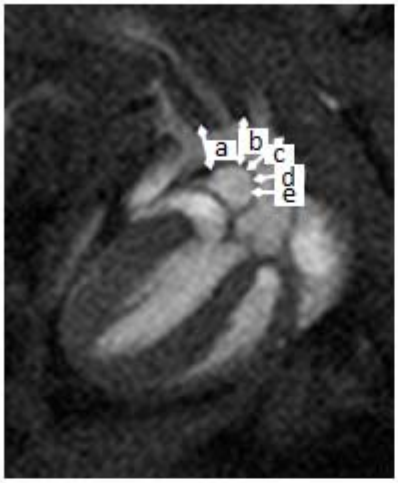

B

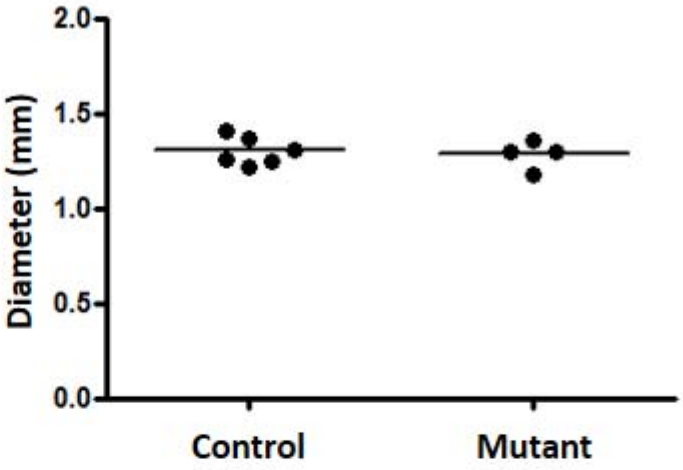

Fig. S6. MRI reveals cardiac dilation and impaired function of postnatal *Prox1* mutant hearts at 6 and 8 weeks. (**A**) Example of a still image from MRI scanned control (*Prox1*$^{fl/fl}$) and mutant (*Nkx2.5*$^{Cre/+}$;*Prox1*$^{fl/fl}$) hearts at 6 and 8 weeks (control is shown at 8 weeks) with significant chamber dilation and thrombus formation in the mutants at 8 weeks, as determined by late gadolinium enhancement (LGE). Scale bar 1 mm. (**B**) left ventricular (LV) ejection fraction (EF) and LV mass normalised to body weight (nLVM) data collected from control and mutant animals at 6 weeks of age indicating significantly impaired cardiac function, via reduced LV EF (below the 45% threshold for DCM) and elevated nLVM in mutants versus age-matched controls (**B**). N=6; **p≤0.01; ****p≤0.0001, significance determined by Student's t-test in comparison to control levels at each stage.

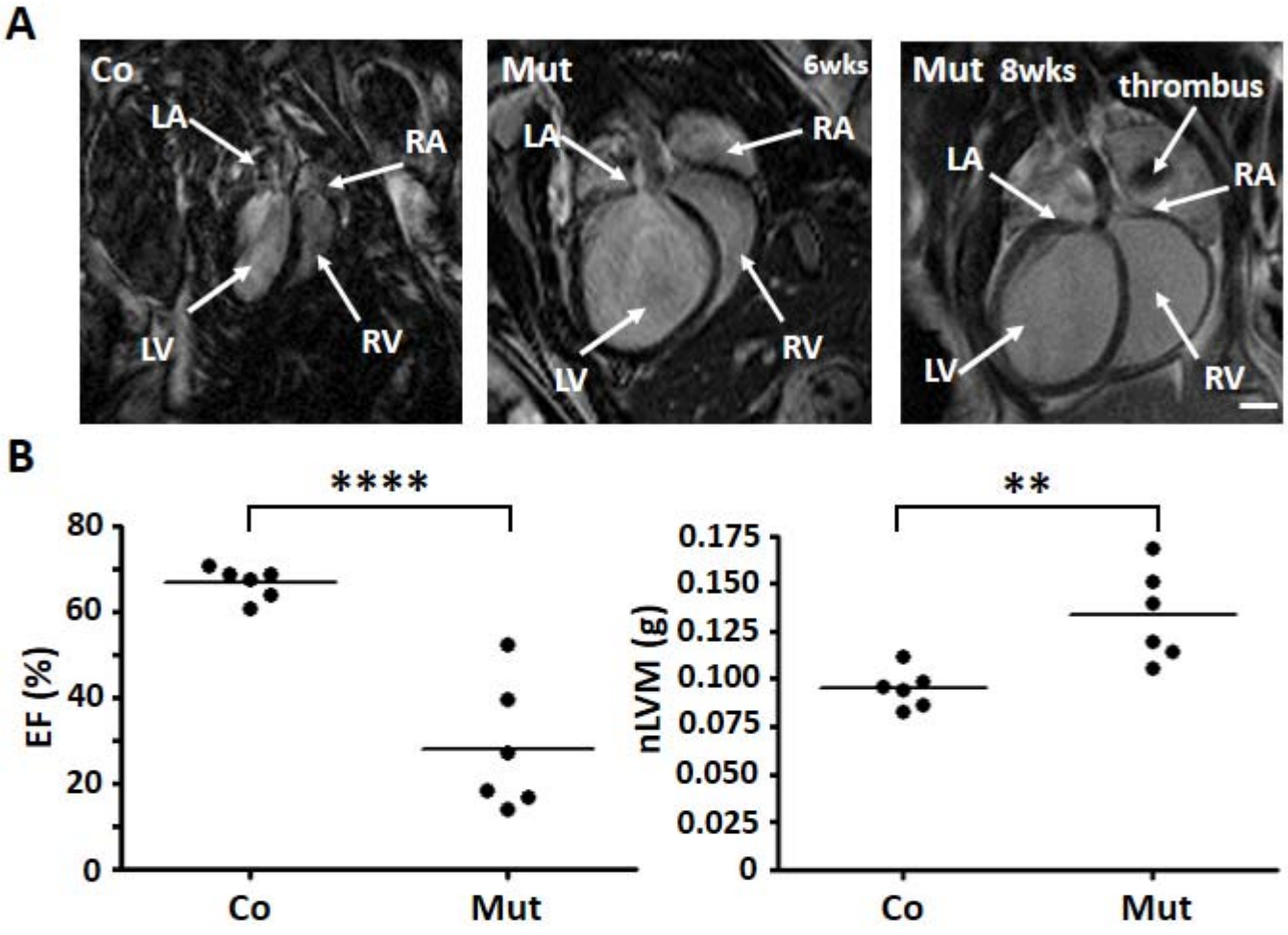
A
Co
LA
RA
LV
RV
Mut
6wks
LA
RA
LV
RV
Mut 8wks
thrombus
LA
RA
LV
RV
B
****
EF (%)
80
60
40
20
0
Co
Mut
**
nLVM (g)
0.175
0.150
0.125
0.100
0.075
0.050
0.025
0
Co
Mut

Fig. S7. Quantification of α-*MHC* transcripts in control (Co, *Prox1*$^{fl/fl}$), cre (Cre, *Nkx2.5*$^{Cre/+}$*;Prox1*$^{+/+}$), heterozygous (Het, *Nkx2.5*$^{Cre/+}$*;Prox1*$^{fl/+}$), and mutant (Mut, *Nkx2.5*$^{Cre/+}$*;Prox1*$^{fl/fl}$) hearts at E12.5 (N=3) and 4 (N=2), 8 (N=3), and 12 (N=2) weeks. Data expressed relative to E12.5 control with significance determined by Student's t-test in comparison to control levels at each stage; *p≤ 0.05.

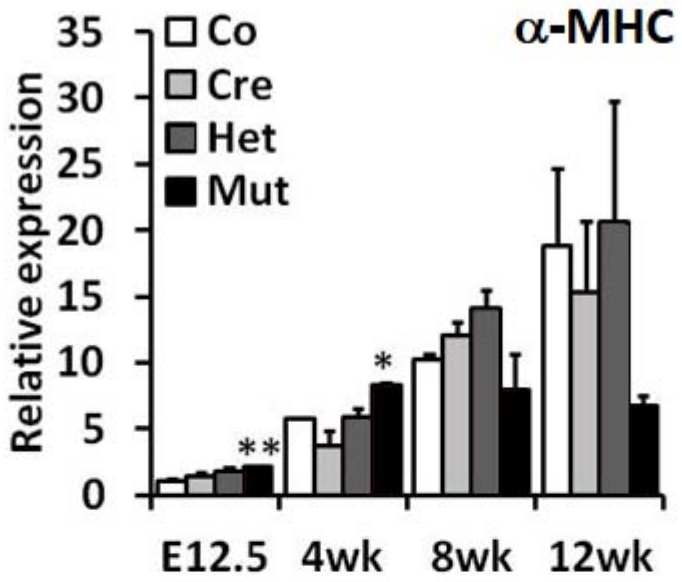
α-MHC
Co
Cre
Het
Mut
Relative expression
35
30
25
20
15
10
5
0
**
*
E12.5
4wk
8wk
12wk

Fig. S8. Sarcomeric structure is unaffected in *Prox1* mutant skeletal muscle. Immunostaining for α-actinin on sections from wild-type (Co) and mutant (Mut) slow-twitch soleus (slow) and fast-twitch EDL (fast) muscles reveals an appropriately striated pattern of α-actinin localisation that is comparable between control and mutant muscles. Scale bar 5 μm.

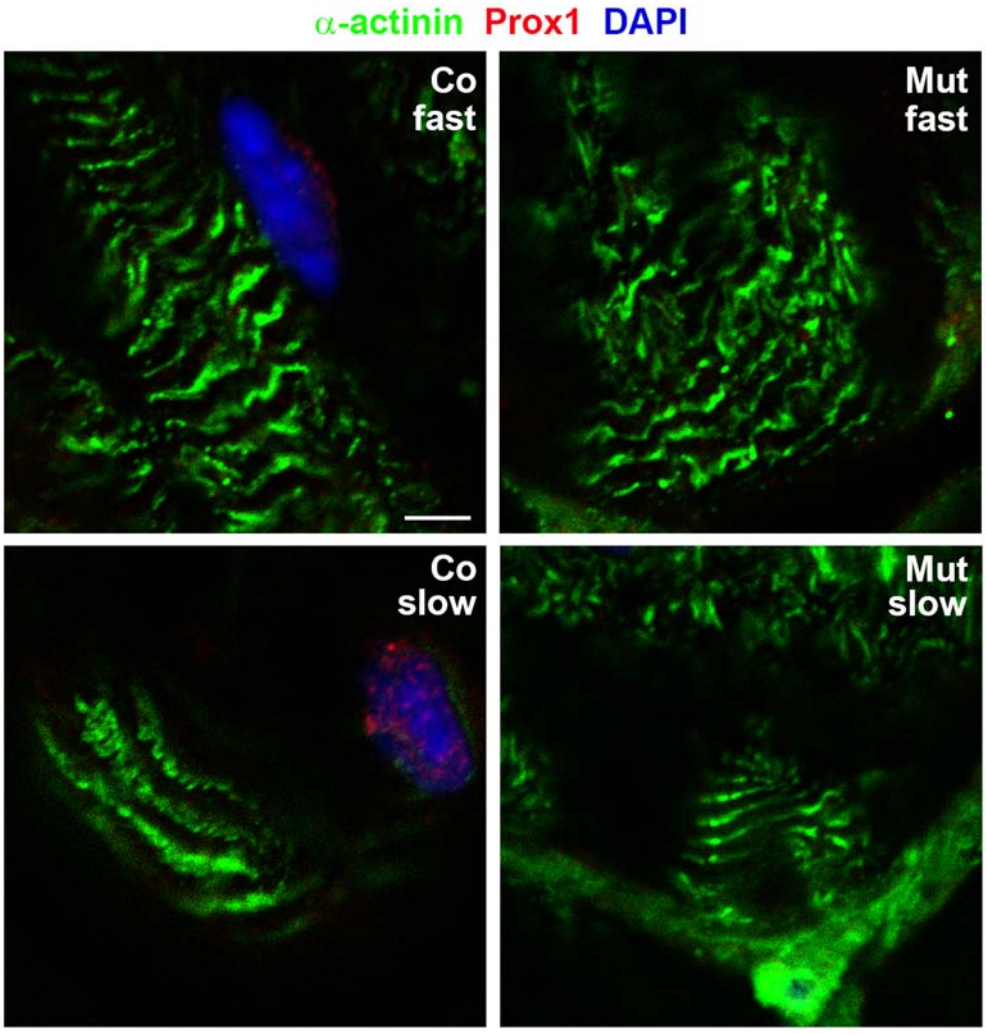
α-actinin Prox1 DAPI
Co
fast
Mut
fast
Co
slow
Mut
slow

Fig. S9. Myosin heavy chain isotype expression. **(A)** Immunostaining for Type I, IIa and IIb myosin heavy chain isotypes on sections from wild-type (Co) and mutant (Mut) slow-twitch soleus (slow) and fast-twitch EDL (fast) muscles. Type IIx expression is revealed by exclusion of positive staining i.e. black fibers. Type IIx expression is increased in mutant slow-twitch muscle compared to control, as indicated by the white arrows. (**B**) Immunostaining for Type I or Type IIa myosin heavy chain on sections showing equivalent expression levels between control (Co) and mutant (Mut) EDL (fast) muscles.

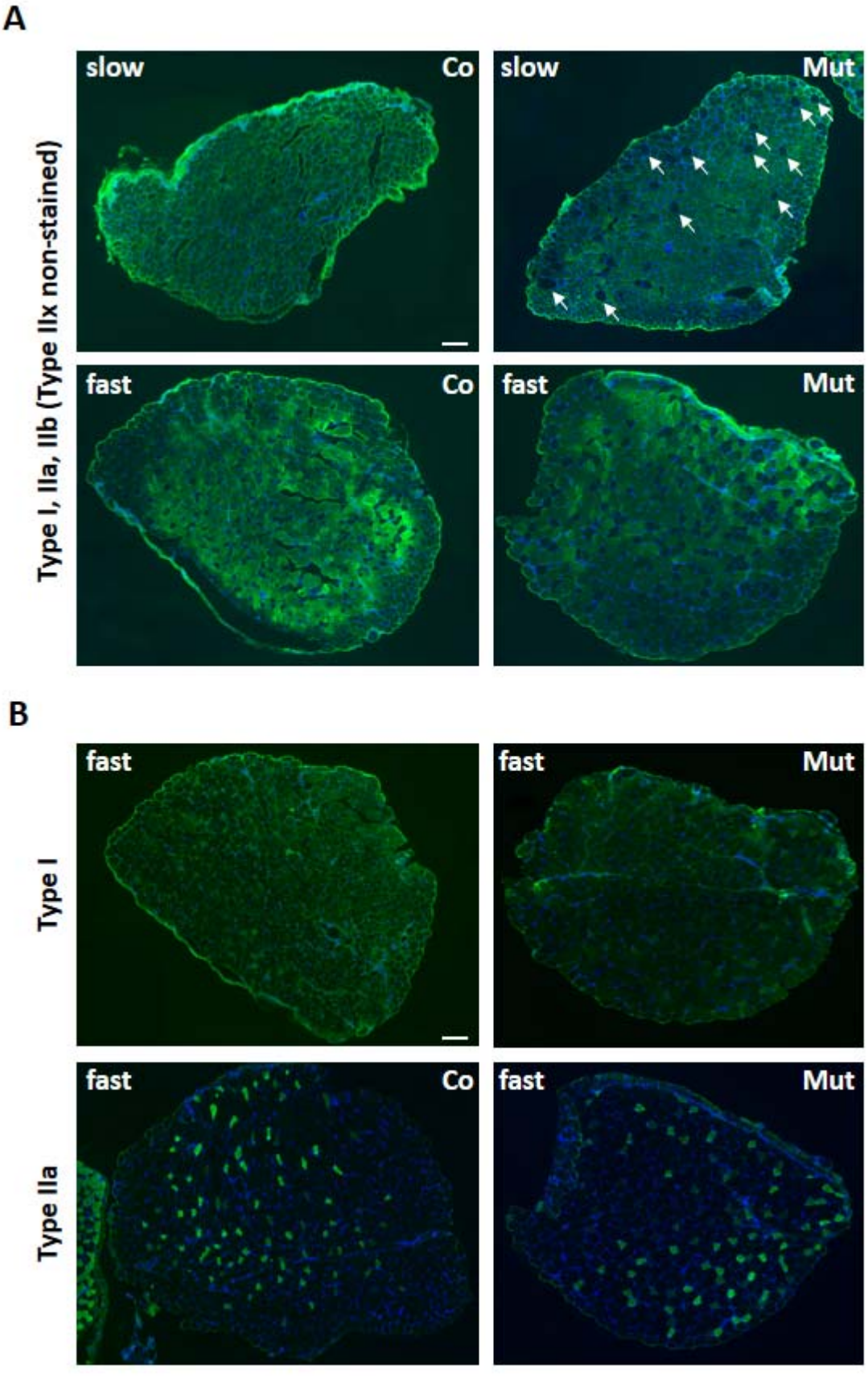
A
Type I, IIa, IIb (Type IIx non-stained)
slow
Co
slow
Mut
fast
Co
fast
Mut
B
Type I
fast
fast
Mut
Type IIa
fast
Co
fast
Mut

Fig. S10. Confirmation of myosin heavy chain isotype switch. (**A**) Silver staining of high resolution polyacrylamide glycerol gels and (**B**) western blotting on slow-twitch soleus and fast-twitch gastrocnemius (gastroc.) muscle lysates confirms upregulation of Type IIa and downregulation of Type I in mutant soleus muscles. There were no observed changes in myosin heavy chain isotype expression in fast-twitch EDL muscles.

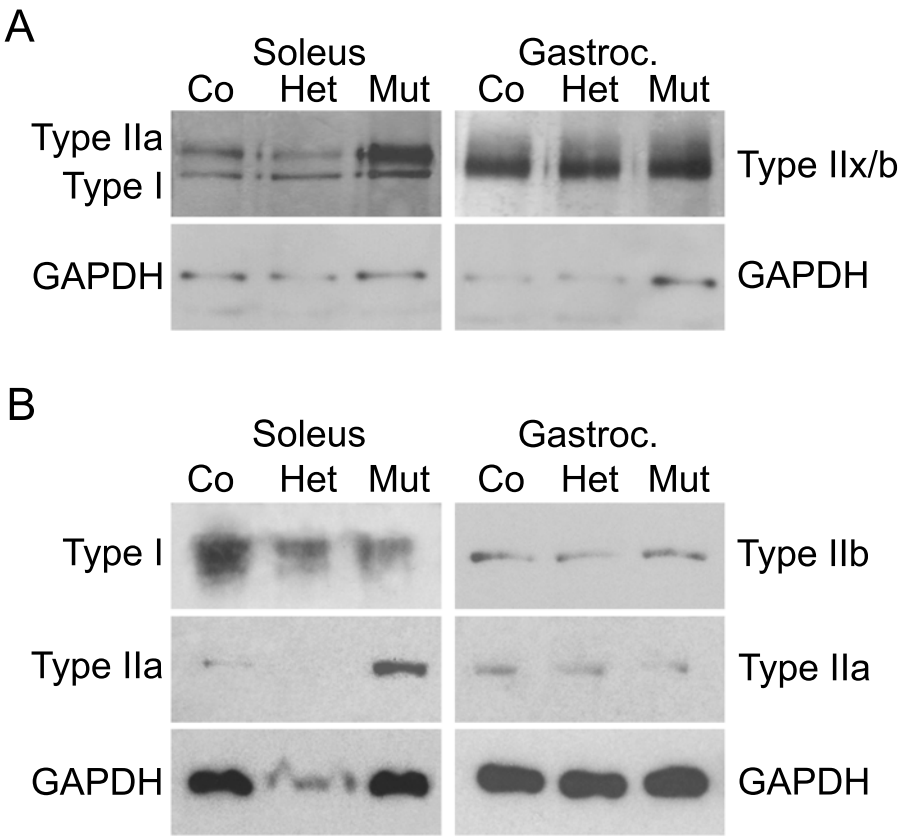
A
Soleus
Gastroc.
Co
Het
Mut
Co
Het
Mut
Type IIa
Type I
Type IIx/b
GAPDH
GAPDH
B
Soleus
Gastroc.
Co
Het
Mut
Co
Het
Mut
Type I
Type IIb
Type IIa
Type IIa
GAPDH
GAPDH

Fig. S11. Myofiber size differs in mutant skeletal muscles. (**A**) Wheat germ agglutinin-Alexa594 staining of control (Co) and mutant (Mut) fast- and slow-twitch muscle sections and (**B**) quantification of myofiber size, analysed in ImageJ. Myofibers were significantly smaller in *Prox1* mutant slow-twitch soleus muscles and larger in mutant fast-twitch EDL muscles. Significance determined by Student's t-test in comparison to control, ****p≤0.0001. Scale bar 20 μm.

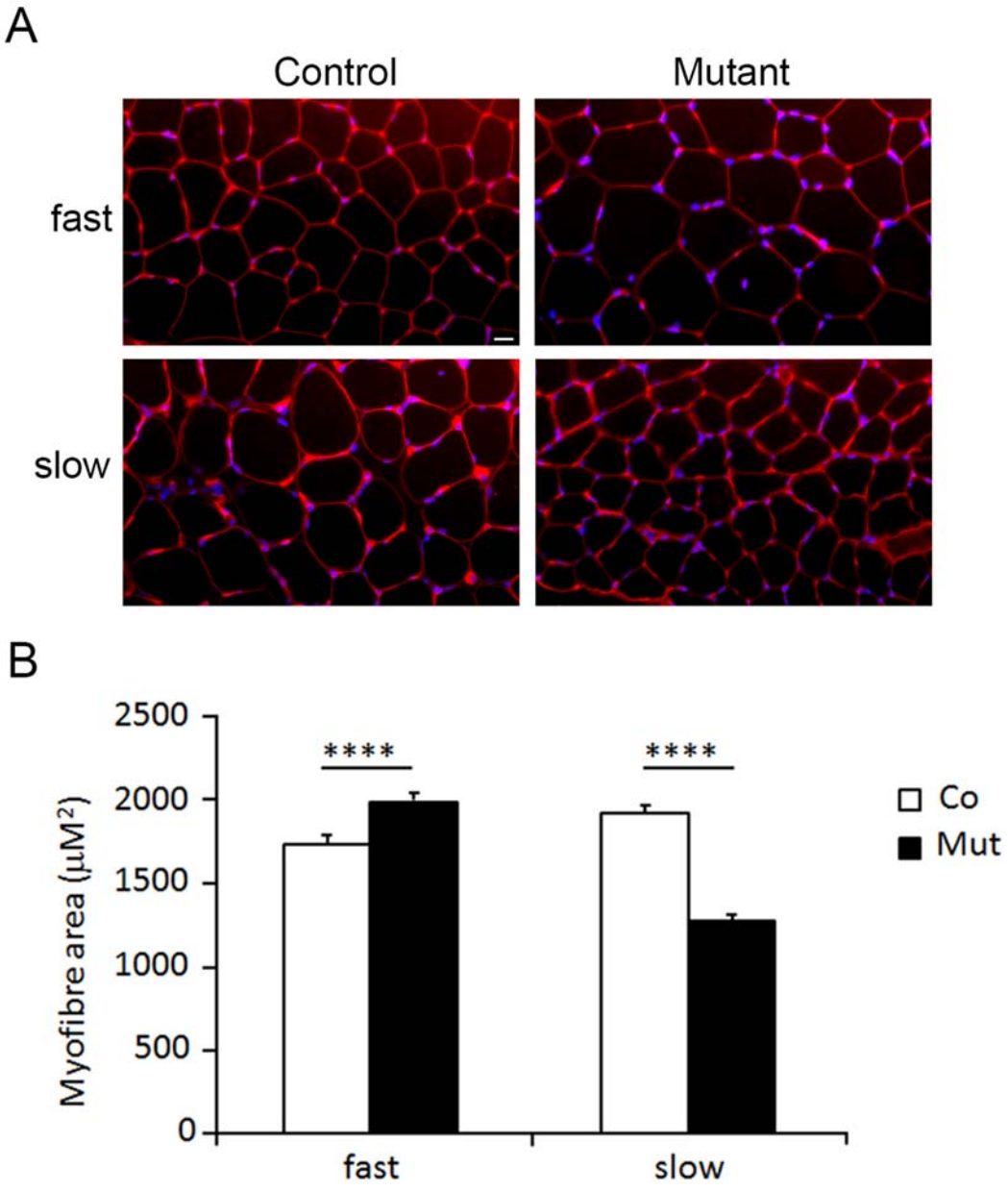
A
Control
Mutant
fast
slow
B
2500
2000
1500
1000
500
0
Myofibre area (µM²)
****
****
Co
Mut
fast
slow

Fig. S12. Overall oxidative capacity is equivalent between mutant and control skeletal muscles. Succinate dehydrogenase staining was performed on sections from control (Co) and mutant (Mut) slow-twitch soleus (sol) and fast-twitch EDL muscles. Overall oxidative capacity was estimated using ImageJ and was found to be equivalent in all muscles. Scale bar 50 μm.

A

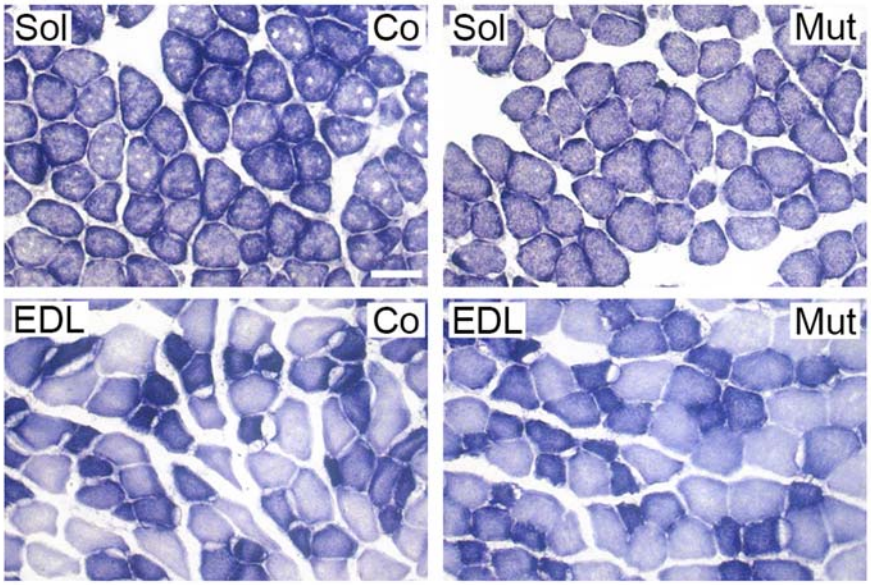
Sol
Co
Sol
Mut
EDL
Co
EDL
Mut

B

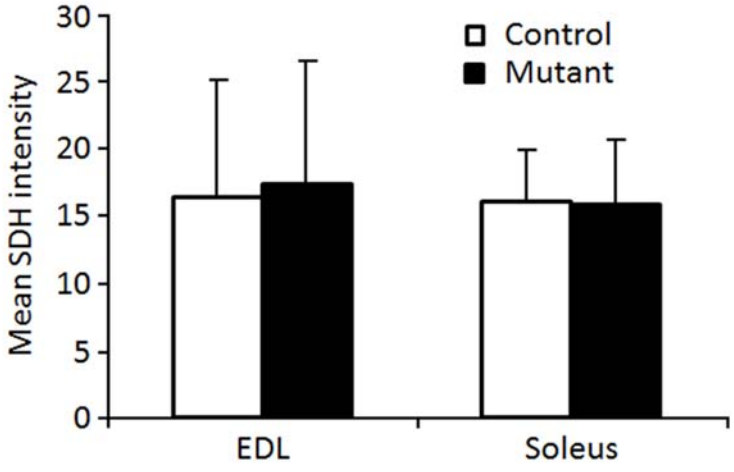
Mean SDH intensity
30
25
20
15
10
5
0
Control
Mutant
EDL
Soleus